Supplemental Information

Liver environment-imposed constraints diversify movement strategies of liver-localized CD8 T cells

Harshana Rajakaruna, James O'Connor, Ian A. Cockburn, Vitaly V. Ganusov

Additional movies, figures, and tables

Movie S1: Example of movement of liver-localized CD8 T cells with labeled liver sinusoids. Experiments were performed as described in Fig. 1 in 3 individual mice. In the movie red denotes rhodamine dextran-labeled liver sinusoids and green are *Plasmodium*-specific liver-localized CD8 T cells (OT-I). Cells turn yellow when there is an overlap between green and red. Bar scale is 50 μm. The volume of $512 \times 512 \times 44$ μm was scanned every 13 sec.

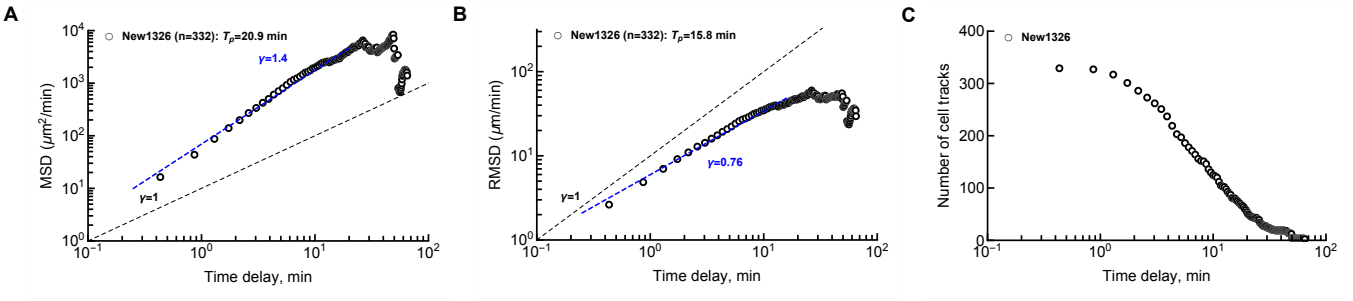

Figure S1: Departure from linear (on log-log scale) change in MSD or root mean squared displacement (RMSD) is in part due to decline in the number of cells with long tracks. For the New1326 datasets of activated CD8 T cells in the liver we calculated the MSD (panel A), RMSD (RMSD = $\sqrt{\text{MSD}}$, panel B), or the number of T cell tracks used to calculate these characteristics (panel C). Note that panel A lists a different slope from that given in Fig. 2A because different number of data points are taken into account in regression (T_p is the persistence time defining which data points were taken for linear regression).

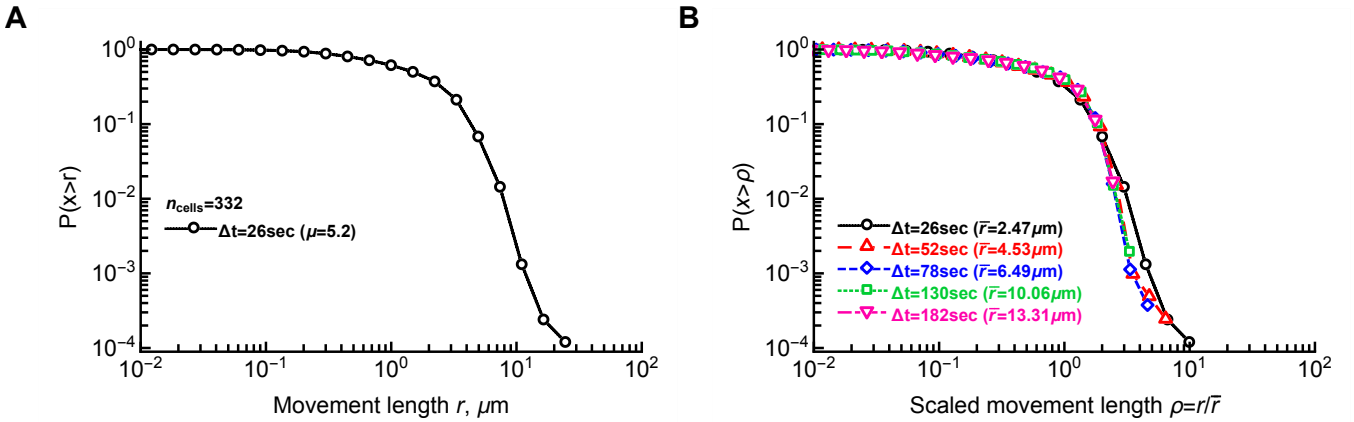

Figure S2: Liver-localized display similar displacement distribution for sub-sampled data. For the cleaned New1326 dataset we calculated the cumulative distribution of displacements for all data (panel A) or when we sub-sample the data, i.e., by taking every time frame ($\Delta t = 26$ sec), every second time frame ($\Delta t = 52$ sec), etc (panel B). In panel B we rescaled all displacements by the average displacement $\bar{r}$ in a given sub-sampled dataset. Results were similar if we scaled the data by dividing displacements by the relative duration of the sub-sampling period ($k = 1, 2 \ldots$). Parameter μ in panel A is from the fit of the Pareto distribution (with $r_{\min} = 9.1$ μm) to the subset of the data (fail fit in which data with $r \geq r_{\min}$ were used).

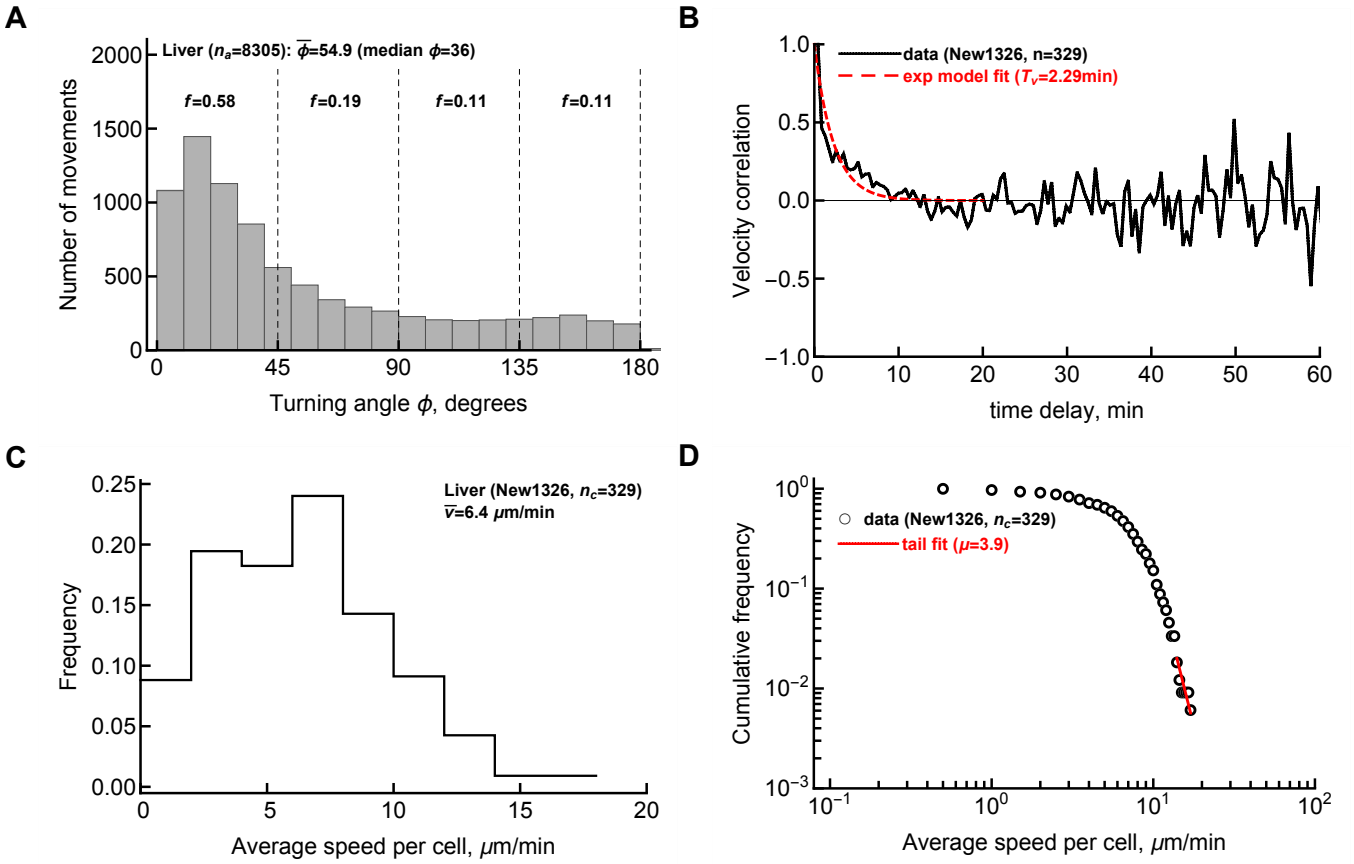

Figure S3: Activated CD8 T cells in the liver perform correlated random walk with a high degree of persistence. A: For every track in our dataset that includes measurement of T cell movement in the liver at 26 sec time steps, we calculated the turning angles for each subsequent cell movement. The data are from 3 individual mice involving 332 cleaned tracks and 8305 movements ("New1326" dataset). Fraction f denotes the frequency of turning angles between specific cutoff values. B: We calculated the correlation between vectors determining the first movement and every another movement for all 329 cell tracks in our data for which velocity correlations could be calculated. Specifically, we calculated the angle ϕ between the vector determining the first cell movement and every another movement at different times and plotted $\cos(\phi)$ vs. the time difference between first movement and another movements. Insert in B shows the data for the first 20 min of imaging. The exponential decay model ($v = v_0 e^{-t/T_v}$ was fitted to the data and estimated parameter T_v is shown. C: Distribution of average speed per cell in these data. D: cumulative distribution of speeds of all cells int he population. Parameter μ denotes the shape parameter of the Pareto distribution fitted to the tail of these data.

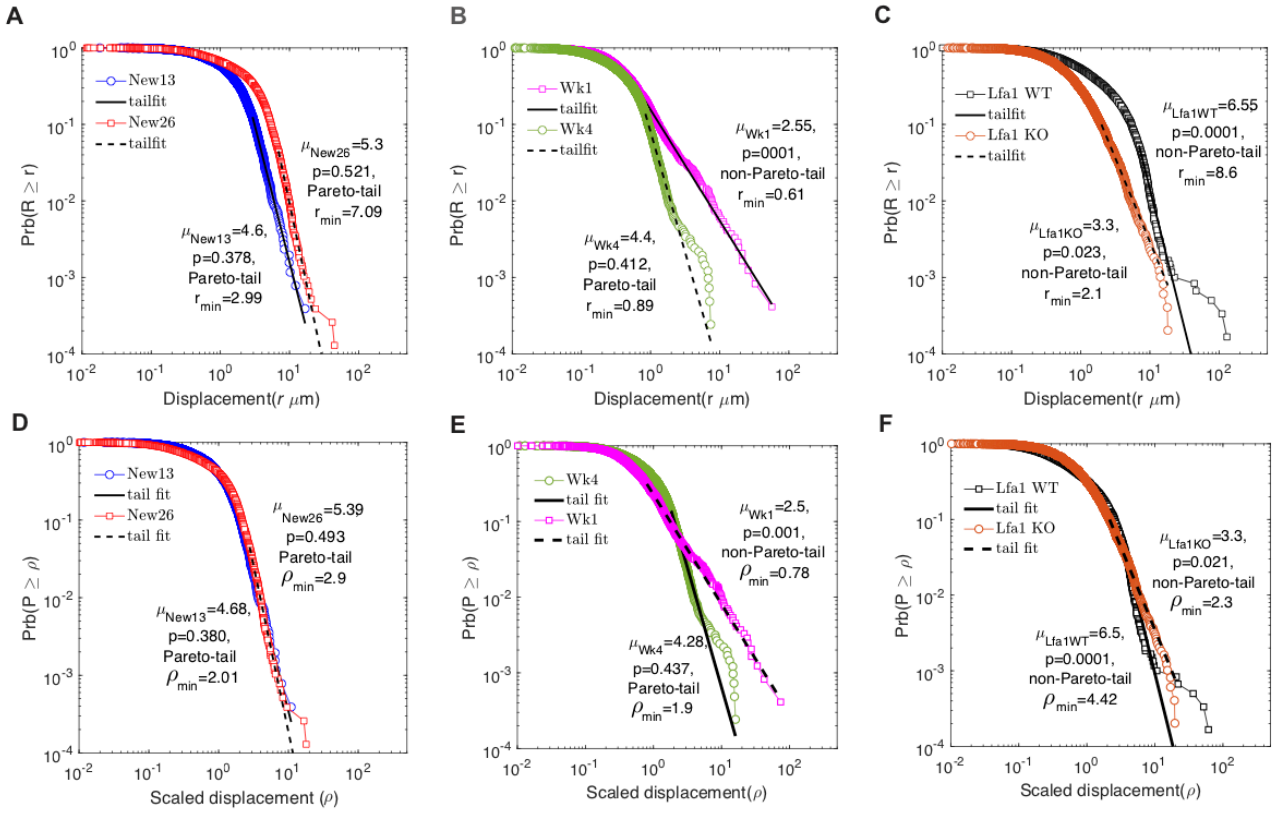

Figure S4: Fits of the Pareto (powerlaw) distributions to the CD8 T cell in the liver displacement data. We used previously published method [34] to estimate the shape parameter μ of the Pareto distribution (eqn. (9)) for 6 different datasets (see Materials and Methods for dataset description) by fitting a linear function (on log-log scale) to the tails of the data distribution using likelihood method. We fit the model to actual displacements r (A-C) or to scaled displacements ρ (D-F). The cut-off $r_{\min}$ (for actual displacements) or $\rho_{\min}$ (for normalized displacements) for the linear regressions was chosen using a goodness-of-fit based method [34]. In short, for multiple choices of $r_{\min}$ slope μ was estimated via the method of maximum likelihood and the Kolmogorov-Smirnov goodness of fit statistic, D, was calculated. Value of $r_{\min}$ that resulted in minimal fit statistics D was chosen for the final fit. Indicated p values were estimated by resampling the data 1000 times and performing Kolmogorov-Smirnov Goodness of Fit Test [34].

Non-scaled data	Dataset	Levy γ	Cauchy γ	GP k	GP σ	Exp λ	H-N σ	Pareto r_{min} (mm)	Pareto μ-tail	Sampling frequency (sec)
Liver	New13	0.35	1.14	-0.07	1.64	1.53	2.01	3.03	4.63	13.00
Liver	New26	0.48	1.69	0.00	2.51	2.50	3.50	7.09	5.32	26.00
Liver	New1326	0.49	1.69	-0.01	2.51	2.49	3.46	7.09	5.47	26.00
Liver	Wk1	0.13	0.40	0.28	0.50	0.76	2.15	0.61	2.55	6.50
Liver	Wk4	0.10	0.33	0.01	0.46	0.46	0.66	0.94	4.42	3.25
Liver	Lfa1_WT	0.33	1.11	0.18	1.68	2.03	3.11	8.60	6.55	27.50
Liver	Lfa1_KO	0.18	0.57	0.11	0.80	0.91	1.46	2.10	3.30	27.50
LN	0209_Doc6	2.31	7.01	-0.19	10.14	8.72	10.58	22.02	6.67	20.00
LN	0409_Doc7	1.20	3.67	-0.48	5.77	4.16	4.71	6.14	6.74	20.00
Scaled data	Dataset	Levy γ	Cauchy γ	General Pareto k	General Pareto σ	Exp λ	H-N σ	Pareto r_{min}	Pareto μ-tail	Sampling frequency (sec)
Liver	New13	0.23	0.74	-0.07	1.07	1.00	1.31	2.01	4.68	13.00
Liver	New26	0.19	0.68	0.00	1.01	1.00	1.41	2.90	5.39	26.00
Liver	New1326	0.20	0.68	-0.01	1.01	1.00	1.39	2.91	5.55	26.00
Liver	Wk1	0.17	0.52	0.28	0.66	1.00	2.82	0.78	2.52	6.50
Liver	Wk4	0.22	0.71	0.01	0.99	1.00	1.44	1.93	4.28	3.25
Liver	Lfa1_WT	0.16	0.55	0.18	0.83	1.00	1.53	4.42	6.47	27.50
Liver	Lfa1_KO	0.20	0.63	0.11	0.88	1.00	1.60	2.29	3.30	27.50
LN	0209_Doc6	0.29	0.87	-0.38	1.30	1.00	1.14	2.05	9.34	20.00
LN	0409_Doc7	0.29	0.88	-0.48	1.39	1.00	1.13	1.55	7.00	20.00
Structure data	Dataset	Levy γ	Cauchy γ	GP k	GP σ	Exp λ	H-N σ	Pareto r_{min} (mm)	Pareto μ-tail	
Liver sinusoids	Evans Blue	3.48	10.54	-0.20	15.71	13.38	16.37	36.36	7.45	
LN FRCs	CCL19day5	2.31	7.01	-0.19	10.14	8.72	10.58	22.02	6.67	

Table S1: Estimates of parameters providing best fits of various datasets. We fitted Levy (eqn. (6)), Cauchy (eqn. (4)), General Pareto (eqn. (7)), exponential (eqn. (8)), or half-normal (eqn. (5)) to the data on movement of T cells in the liver, lymph nodes, or to branch length distribution data for liver sinusoids or fibroblastic retricular cell (FRC) network in lymph nodes. For distribution with a location parameter $r_{\min}$ we set $r_{\min} = 0$. The same models were also fitted to scaled data (step length distribution data scaled by the RSMD). For imaging data we also list frequency of the imaging in the movies. See Extended Materials and Methods for the models and how models were fit to data. The data are for Plasmodium-specific activated/memory CD8 T cells in the liver (OT1) or naive CD8 T cells in the LNs (P14).

Non scaled data	Dataset	AIC					Akaike Weights				
		Levy	Cauchy	GP	Exp	H-N	Levy	Cauchy	GP	Exp	H-N
Liver	New13	11397	11433	7269	7302	7279	0.00	0.00	0.99	0.00	0.01
Liver	New26	40929	41951	29623	29621	30631	0.00	0.00	0.32	0.68	0.00
Liver	New1326	45728	46801	33002	33003	33968	0.00	0.00	0.58	0.42	0.00
Liver	Wk1	5868	5968	2746	3398	6955	0.00	0.00	1.00	0.00	0.00
Liver	Wk4	8184	8275	1860	1859	2575	0.00	0.00	0.39	0.61	0.00
Liver	Lfa1_WT	26909	28181	19649	19789	21556	0.00	0.00	1.00	0.00	0.00
Liver	Lfa1_KO	15307	15615	8554	8668	10549	0.00	0.00	1.00	0.00	0.00
LN	0209_Doc6	42313	41380	28946	30515	28685	0.00	0.00	0.00	0.00	1.00
LN	0409_Doc7	3352	3278	2281	2433	2281	0.00	0.00	0.53	0.00	0.47
Scaled data	Dataset	AIC					Akaike Weights				
		Levy	Cauchy	GP	Exp	H-N	Levy	Cauchy	GP	Exp	H-N
Liver	New13	9219	9254	5090	5123	5099	0.00	0.00	0.99	0.00	0.01
Liver	New26	26806	27820	15491	15489	16494	0.00	0.00	0.32	0.68	0.00
Liver	New1326	30021	31086	17287	17287	18248	0.00	0.00	0.59	0.41	0.00
Liver	Wk1	7141	7242	4020	4673	8231	0.00	0.00	1.00	0.00	0.00
Liver	Wk4	14498	14595	8181	8180	8901	0.00	0.00	0.41	0.59	0.00
Liver	Lfa1_WT	18723	19988	11456	11596	13359	0.00	0.00	1.00	0.00	0.00
Liver	Lfa1_KO	16191	16499	9439	9554	11435	0.00	0.00	1.00	0.00	0.00
LN	0209_Doc6	24765	23829	11394	12965	11133	0.00	0.00	0.00	0.00	1.00
LN	0409_Doc7	1924	1849	853	1005	853	0.00	0.00	0.54	0.00	0.46
Structure	Dataset	Levy	Cauchy	GP	Exp	H-N	Levy	Cauchy	GP	Exp	H-N
Liver sinusoids	Evans Blue	47544	47114	37936	38375	37599	0.00	0.00	0.00	0.00	1.00
LN FRCs	CCL19day5	29759	29402	23058	23349	22758	0.00	0.00	0.00	0.00	1.00

Table S2: AIC values and Akaike weights of alternative models fit to different datasets (as described in Tab. S1). See Extended Materials and Methods for the models and how models were fit to data.

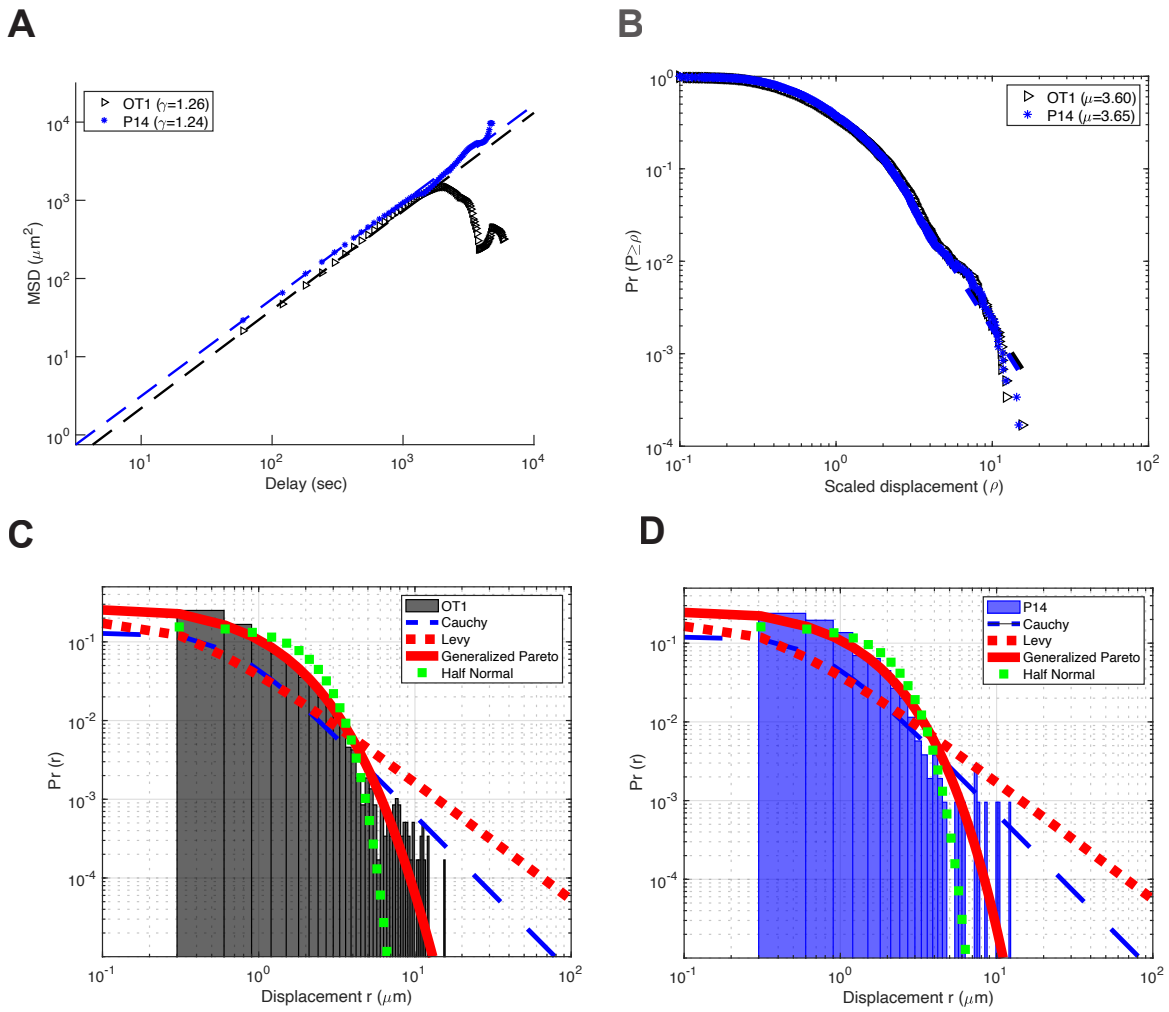

Figure S5: Activated CD8 T cells are superdiffusive Brownian walkers in the liver during *Plasmodium* infection. We performed experiments in which *in vitro* activated OT-I (*Plasmodium berghei*-specific) and P14 (LCMV-specific) CD8 T cells were transferred i.v. into naive mice and these mice were 1.5-2 hours later infected with 10^5 *Plasmodium berghei*-CS^{5M} sporozoites expressing SIINFEKL epitope from chicken ovalbumin [31, 64]. Ten to twenty minutes after infection, livers of infected mice were exposed and movements of T cells were recorded using intravital microscopy [38]. We performed the same analyses as in the main text (Fig. 2) including (A) regression analysis of the MSD with time, (B) distribution of movement lengths, (C)-(D) fitting alternative distributions to the movement data for OT1 (C) or P14 (D) T cells. Generalized Pareto distribution was best describing data in C-D (results not shown).

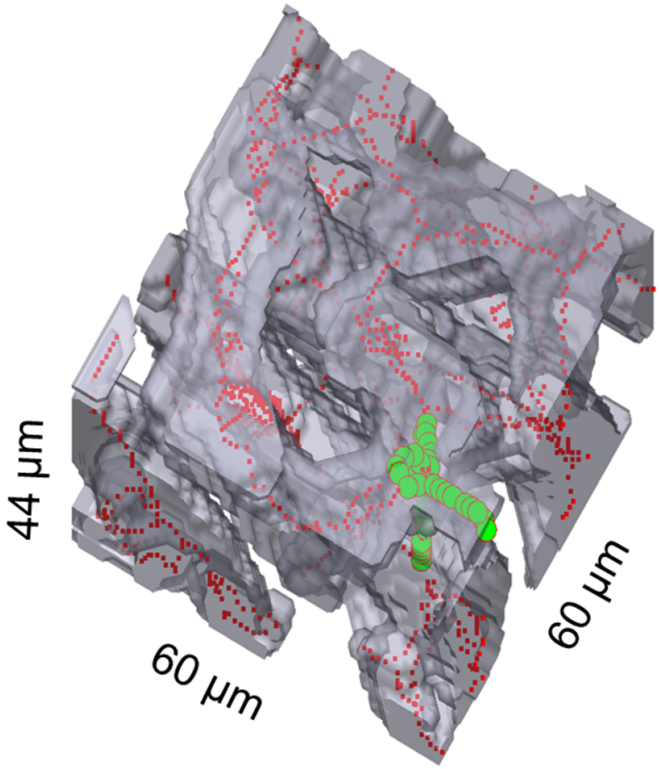

Figure S6: Example of the simulation in which T cells were moving in sinusoids of the liver. Grey denotes sinusoids, red dots denote the mean path of the sinusoids, and green denotes moving T cell.

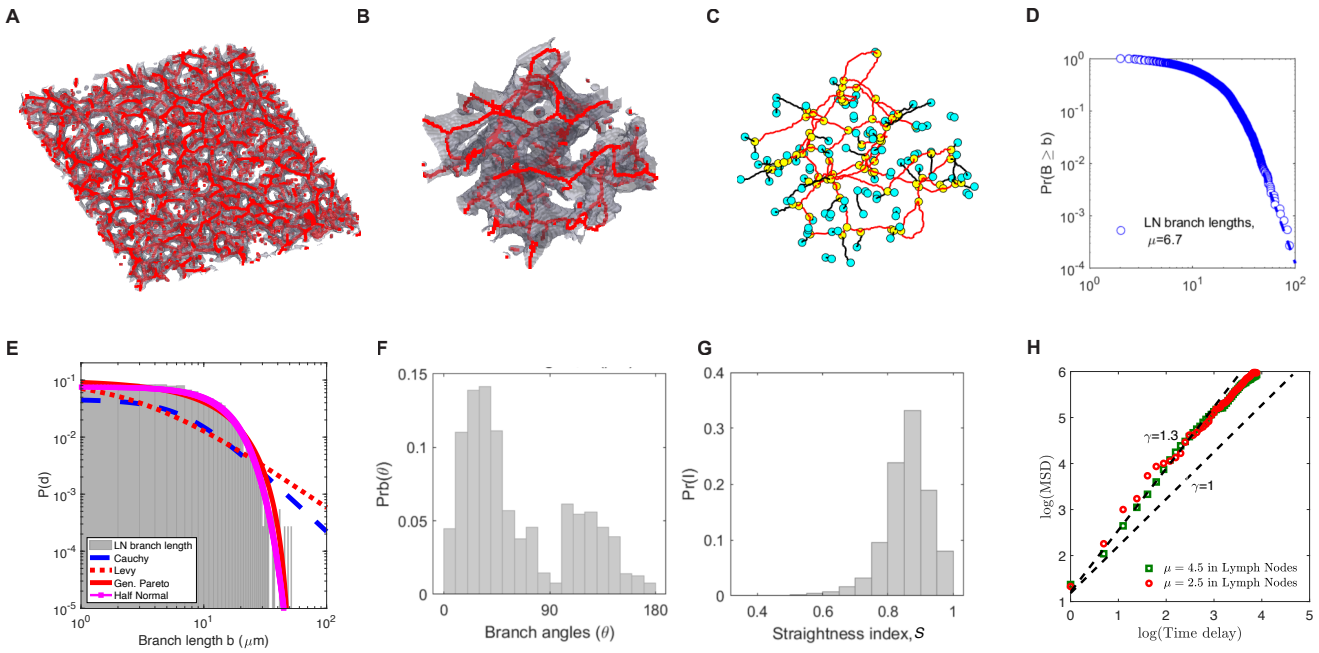

Figure S7: Characterizing structure of the fibroblastic reticular cell network in the murine lymph nodes. We used previously published data in which FRCs were imaged using Ccl19$^{\text{eyfp}}$ reporter mouse [39]. As with analysis of liver sinusoids z-stacks of LN images were contrasted and mean paths in the FRCs were calculated. To simulate T cell walk on digitized FRC network we assumed that movement length distribution is described by the powerlaw (Pareto) distribution with $r_{\min} = 0.2$ μm and $\mu = 4.5$ (for Brownian walks) or $\mu = 2.5$ (for Levy walks).

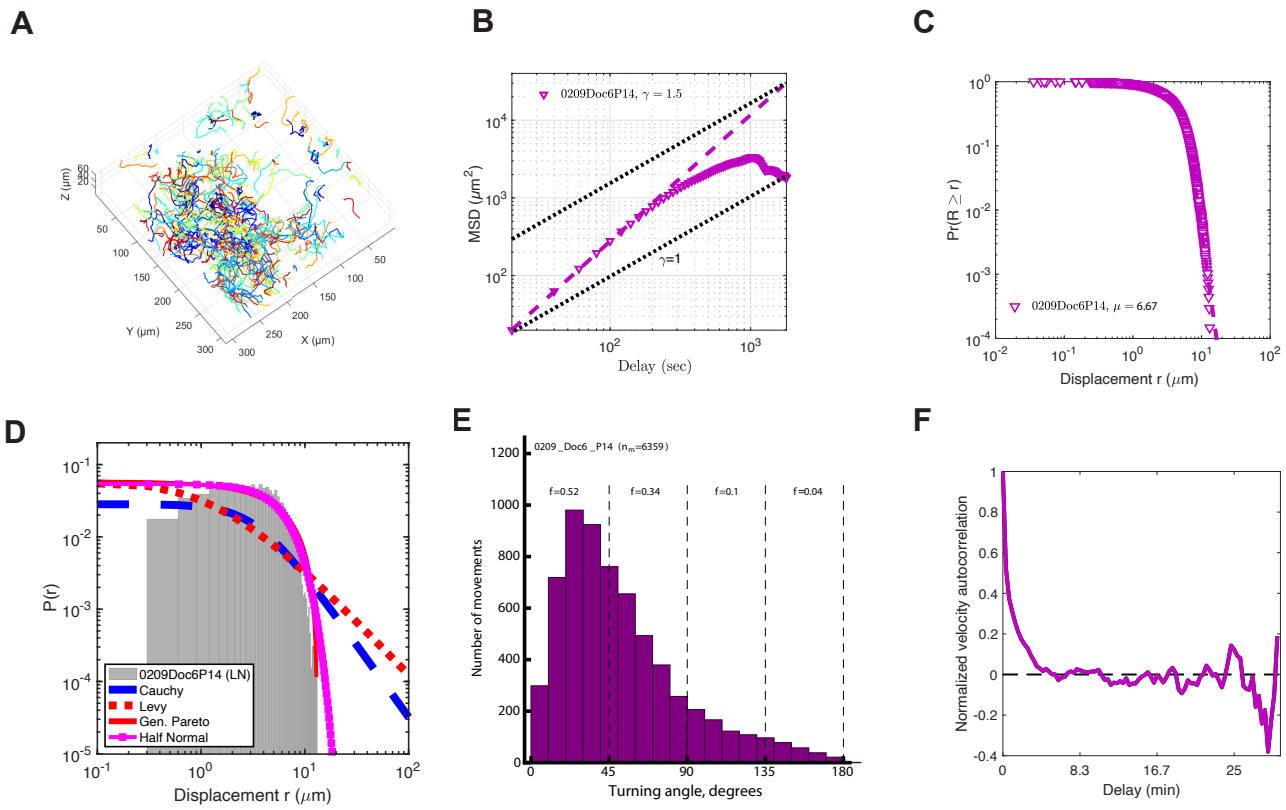

Figure S8: Naive CD8 T cells in lymph nodes are not superdiffusive. We analyzed experimental data in which naive CD8 T cells moving in resting lymph nodes were imaged using two photon microscope [39]. Example of the analysis of data from one of 6 such datasets is show. A: individuals tracks of T cells digitized using Imaris software; B: MSD vs. time for all T cels indicating short-term (2-3 min) persistence/superdiffusion; C: movement length distribution with tail analysis performed [34]; D: fits of several alternative distributions to the movement length distribution data; E: distribution of turning angles of T cells in the LNs; F: velocity autocorrelation function for T cells moving in the LNs.

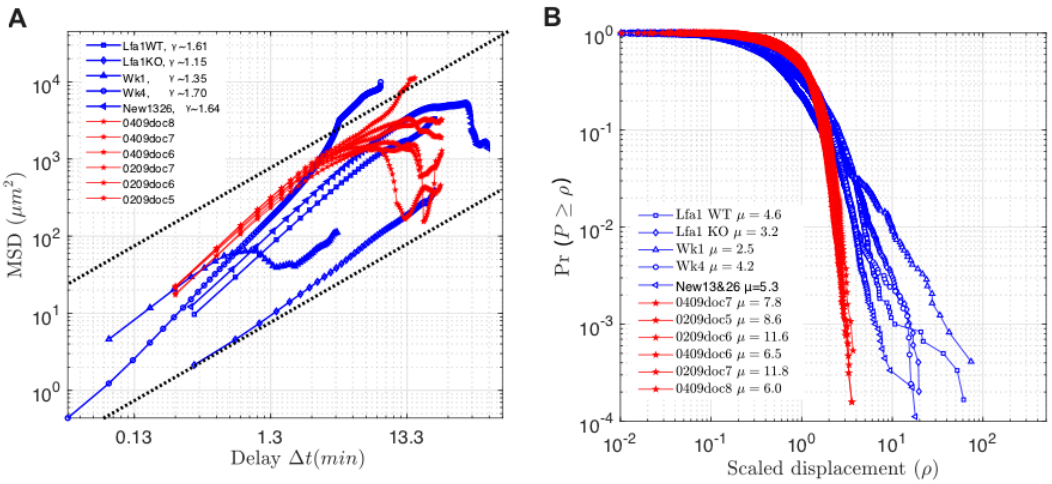

Figure S9: T cells in the liver display persistent movement for a longer time as compared to T cells in the LNs. Data from all datasets on movement of activated CD8 T cells in the liver (blue) or naive CD8 T cells in the LNs (red) are plotted together. A: difference in MSD for T cells in the LNs vs. liver; B: difference in movement length distribution of T cells in the liver vs. LNs.